

GCES OFFICE COPY
DO NOT REMOVE!

SEEPAGE EROSION FROM DAM-REGULATED FLOW: CASE OF GLEN CANYON DAM, ARIZONA

By Muniram Budhu¹ and Roger Gobin²

ABSTRACT: Seepage erosion—in particular, slope failures (bank slumps, mass wasting)—is prevalent on most sandbars downstream from the Glen Canyon Dam, Ariz. The public is concerned about the loss of the extant biomass and recreational facilities on these sandbars. It is alleged that the operation of the Glen Canyon Dam is responsible for the erosion of the sandbars. In this contribution, a simple, approximate analysis is developed to determine the extent of slope failures due to seepage of bank stored water from transient dam flow. The analysis is intended to assist environmentalists, dam operators, planners, and others to predict zones in which riparian habitat and recreation use will be negatively impacted by fluctuating flows. The affected area of a sandbar was found to be dependent on the range of flows; the rate of rise of river stage; the duration of the peak discharge; and the permeability, friction angle, and cohesion of the soil. Comparison of the predictions of the analysis with field data show good agreement.

INTRODUCTION

The Glen Canyon Dam, located in north-central Arizona near the Utah border (Fig. 1), was commissioned in 1963 to provide flood control, water storage and hydroelectric power for some western U.S. states (Stevens 1983). Power demands and, consequently, dam discharge vary during the day, creating a daily tide. Peak dam discharge usually occurs at about the middle of the day. Typical daily river stage fluctuation is 1–3 m with some narrow river sections reaching 4 m.

Before the construction of the Glen Canyon Dam, the unregulated Colorado River was laden with sediments. During periods of heavy precipitation, large volumes of sand, silts and mud were transported by the tumultuous murky flow in the channel. In the postdam era, most of the sediments are trapped upstream of the dam in Lake Powell. The water downstream of the dam is almost clear. Sediment concentration near Lees Ferry was in excess of 10,000 parts per million (ppm) prior to the construction of the dam. Now, the sediment concentration there is about 200 ppm (Schmidt and Graf 1990).

Sandbars are scattered along the banks of the main channel but are more common at the confluences of ephemeral tributaries and the main channel. During floods or high dam releases, deposits at the confluences and fresh sediments from the ephemeral tributaries are transported and then redeposited at locations conducive to aggradation. At these locations, where the velocity is much lower than the average velocity, new sandbars are formed and existing sandbars are either replenished, if prior erosion occurred, or increased in size. These sandbars form a natural environment for riparian habitat and campsites for rafters and hikers.

In the pre-dam era, the mean annual maximum flow was 2,439 (m³/s) with a record flow of 5,660 m³/s in 1921 (Howard and Dolan 1981). The riverbanks were continuously scoured, especially during spring snow melt and periods of heavy precipitation. However, some of the scoured areas were rebuilt during the receding flood because of the large sediment load in the river. Regular scouring of the riverbanks prevented the development of vegetation below the old high water line in the predam period.

The Glen Canyon Dam now regulates the Colorado River with flows varying from 57 m³/s to about 849 m³/s. A lush, vibrant, band of vegetation supporting a rich and diverse riparian life exists along the Colorado River (Turner and Karpiscak 1980). The continued existence of this new riparian habitat is challenged by dam operation. Daily tidal variations in river stage encourage seepage, which results in bank slumps, rilling, and other erosion features on many of the sandbars used for recreation and riparian habitat.

To determine the effects of dam operation on the recreation and riparian environment, the U.S. Bureau of Reclamation initiated the Glen Canyon Environmental Studies program (U.S. Department of the Interior 1988). This contribution is part of the aforementioned study program. During a two-year study period that began in September 1990, three erosion processes—seepage, tractive scour, and wave attack—were identified (Budhu 1992) as the main causes of the erosion

¹Assoc. Prof., Dept. of Civ. Engrg. and Engrg. Mech., Univ. of Arizona, Tucson, AZ 85721.

²Grad. Student, Dept. of Civ. Engrg. and Engrg. Mech., Univ. of Arizona, Tucson, AZ.

Note. Discussion open until July 1, 1995. To extend the closing date one month, a written request must be filed with the ASCE Manager of Journals. The manuscript for this paper was submitted for review and possible publication on December 20, 1993. This paper is part of the *Journal of Irrigation and Drainage Engineering*, Vol. 121, No. 1, January/February, 1995. ©ASCE, ISSN 0733-9437/95/0001-0022-0033/\$2.00 + \$.25 per page. Paper No. 7551.

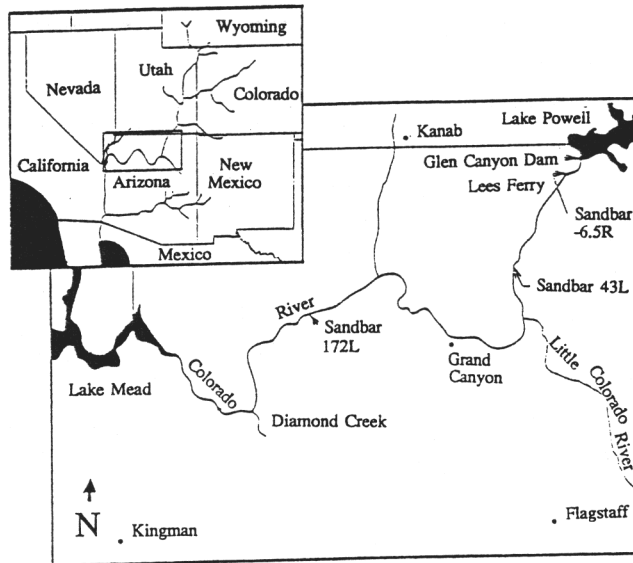


FIG. 1. Study Area



FIG. 2. Typical Coulomb Failure

of sandbars downstream from the Glen Canyon Dam. Of these processes, seepage is ubiquitous. The question that arises is what is the extent of seepage erosion on sandbars that negatively impacts the riparian and recreation environment? In this contribution, an analysis is presented to determine the extent of slope failures (bank slumps, mass wasting) from transient ground-water seepage resulting from dam operation. This analysis could be useful to environmentalists, dam operators, planners, and others in determining the changes in riparian and recreation environment resulting from dam operation.

SEEPAGE EROSION AND OBSERVATIONS IN GRAND CANYON

Erosion by ground-water seepage is described by many terms such as artesian sapping, spring sapping, seepage driven erosion, rilling, seepage-induced transport and seepage weathering. The mechanics of each of these phenomena are slightly different. The term "seepage erosion" will be used here to refer to slope failures or bank slumps or mass wasting events from transient ground-water seepage.

Several seepage processes were observed in most of the sandbars downstream from the Glen Canyon Dam. Slope failures are, however, ubiquitous. If the river stage is raised and then lowered faster than the bank-stored water can drain, an excess pore-water pressure will remain within the river bank. At the same time, due to the decrease in river-stage elevation, the

stabilizing water pressure on the sandbar will also be removed. The combined effect of the removal of the stabilizing water pressure, the buildup of excess pore-water pressure and seepage forces results in Coulomb-type slope failures (Fig. 2). Slope failures observed (Cluer 1992) along the Colorado River downstream from the Glen Canyon Dam are usually rapid and very destructive, and involve several hundred cubic meters of soil. A substantial area of a sandbar is destroyed in just a few seconds.

ANALYSIS OF SEEPAGE EROSION IN AN UNSATURATED-SATURATED COHESIONLESS SOIL MASS

Consider an element of soil of unit cross-sectional area at a depth Z below the ground surface in the saturated region. The soil mass is assumed to be a homogenous, stress-free, infinite slope of slope angle α that is subjected to a seepage force per unit area, $i\gamma_w h$, where i is the seepage vector (hydraulic gradient), γ_w is the unit weight of water, and h is the depth of the soil element below the ground-water level. Capillary effects are neglected. The direction of the seepage force is assumed to make an angle λ with the plane normal to slope (Fig. 3). The disturbing force down the slope (T) is

$$T = W \sin \alpha + i\gamma_w h \sin \lambda \quad (1)$$

where W , soil weight per unit area, is

$$W = \gamma D + \gamma' h \quad (2)$$

in which γ = total unit weight; $\gamma' = \gamma_{\text{sat}} - \gamma_w$ = effective unit weight; and γ_{sat} = saturated unit weight of the soil. The resisting force given by Coulomb's failure criterion, for a cohesionless soil, is

$$R = N \tan \phi' \quad (3)$$

where N , the effective normal force, is

$$N = W \cos \alpha - i\gamma_w h \cos \lambda \quad (4)$$

and ϕ' = effective angle of friction. Substituting (4) into (3), we obtain

$$R = (W \cos \alpha - i\gamma_w h \cos \lambda) \tan \phi' \quad (5)$$

The factor of safety of the slope against a Coulomb-type failure is

$$F = \frac{R}{T} = \frac{(W \cos \alpha - i\gamma_w h \cos \lambda) \tan \phi'}{W \sin \alpha + i\gamma_w h \sin \lambda} \quad (6)$$

The maximum seepage effect on slope stability (minimum factor of safety) occurs in (6) when $\sin \lambda = 1$, that is, $\lambda = 90^\circ$. Seepage is then parallel to the slope and $i = \sin \alpha$. At limiting equilibrium, $F = 1$, (6) then reduces further to

$$\tan \phi' = \frac{W \sin \alpha + i\gamma_w h \sin \lambda}{W \cos \alpha - i\gamma_w h \cos \lambda} \quad (7)$$

Substituting (2) into (7) gives, on algebraic simplification

$$\tan \phi' = \frac{\sin \alpha + \left(\frac{i \sin \lambda}{\xi}\right)}{\cos \alpha - \left(\frac{i \cos \lambda}{\xi}\right)} \quad (8)$$

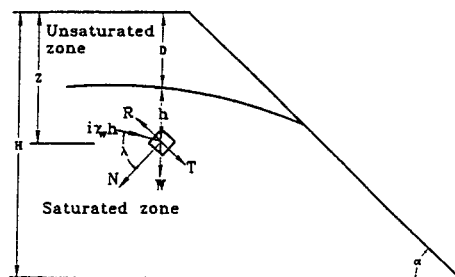


FIG. 3. Forces on Elemental Volume for Saturated-Unsaturated Soil

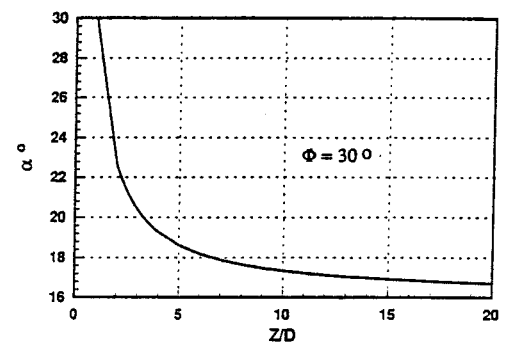


FIG. 4. Plot of Stable Seepage Slope as Function of Z/D Ratio

where

$$\xi = \frac{\gamma D}{\gamma_w h} + \frac{\gamma'}{\gamma_w} \quad (9)$$

and

$$\frac{\gamma}{\gamma_w} = \frac{G + Se}{1 + e}; \quad \frac{\gamma'}{\gamma_w} = \frac{G - 1}{1 + e} \quad (10a,b)$$

where G = specific gravity of the soil; e = void ratio; and S = degree of saturation.

For seepage parallel to the slope ($\lambda = 90^\circ$, $i = \sin \alpha$), (8) reduces to

$$\tan \alpha = \left(\frac{\xi}{1 + \xi} \right) \tan \phi' \quad (11)$$

if the soil mass above the ground-water level is dry, $S = 0$. Assuming $\gamma'/\gamma_w = 1$ (equivalent to $e = 0.7$ for $G = 2.7$), a reasonable assumption for most soils, and $\phi' = 30^\circ$, then

$$\xi = 1.588 \left[\frac{1}{\left(\frac{Z}{D} \right) - 1} \right] + 1; \quad \frac{Z}{D} \geq 1 \quad (12)$$

A plot of the stable seepage slope using (11) and (12) is shown in Fig. 4. From the ground surface to the ground-water level, $Z/D \leq 1$, the slope angle is ϕ' . As Z/D increases, the slope angle decreases rapidly until about $Z/D = 10$, then slowly decreases to $\tan^{-1}(0.5 \tan \phi)$ as $Z/D \rightarrow \infty$. For practical purposes, slopes with $Z/D > 10$ in an unsaturated-saturated cohesionless soil can reasonably be assumed to be infinite.

For a fully saturated slope, $D = 0$, $\xi = \gamma'/\gamma_{sat}$, and for seepage parallel to the slope, (11) reduces to Taylor (1948) equation

$$\alpha_s = \tan^{-1} \left(\frac{\gamma'}{\gamma_{sat}} \tan \phi' \right) \quad (13)$$

where α_s = stable seepage slope for seepage parallel to slope. Iverson and Major (1986) obtained a similar equation to (8) using a differential calculus approach. They assumed a saturated slope in which case, $\xi = \gamma'/\gamma_{sat}$.

APPLICATION OF ANALYSIS TO SANDBARS IN GRAND CANYON

Glen Canyon Dam is operated such that water is discharged at a suitable rate to meet peak power demands, which occur for relatively short intervals (about 2 h). The ground-water level in sandbars rarely equilibrate with the peak river stage. There is also no water source behind the sandbars to maintain constant seepage to provoke continuous slope failures (Howard and McLane 1988).

Consider a sandbar of slope angle ϕ' . Discharge from the dam will cause water to infiltrate into the sandbar, and at peak discharge the ground-water level in the sandbar could be represented by the curve shown in Fig. 5. The ground-water level is dependent on dam operation (rate and magnitude of discharge, and duration of peak) and the soil condition (permeability and homogeneity). If the peak discharge is held for some period of time, the ground-water level will move upwards with point P remaining fixed. The amount of bank-stored ground-water will then increase. If the permeability of the soil increases, then the elevation of the ground-water level will also increase.

We assume here that, within the range of dam discharges from the Glen Canyon Dam, the limiting condition of seepage parallel to the slope will occur in most sandbars. Accordingly, a lower seepage slope (AB) can be defined by a plane of inclination, α , (11), drawn from the lowest water level, intersecting the ground-water level at the highest peak river stage at B (Fig.

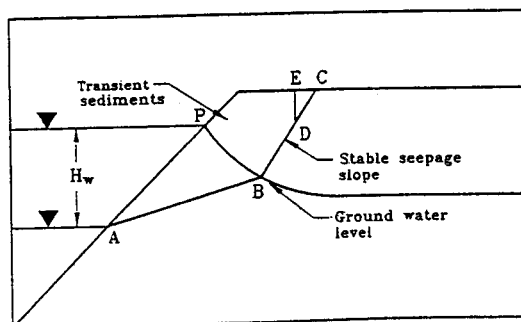


FIG. 5. Stable Seepage Slope

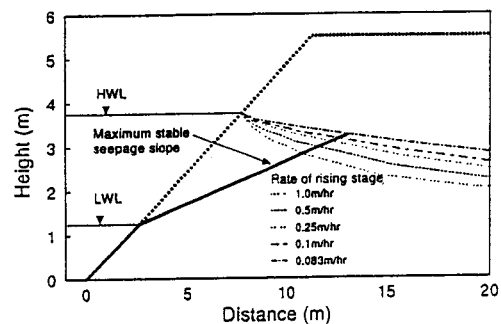


FIG. 6. Variation of Phreatic Surface with Rate of Rising River Stage

5). The stable seepage slope for the portion of the sandbar above the ground-water level (upper seepage slope) would be its angle of internal friction described by a plane BC. On the upper part (about 0.5 m thick) of some sandbars, the sand is mixed with silts and clays imparting a small amount of cohesion (<2 kPa). In these cases, a vertical face (tension crack), ED, of depth (Terzaghi 1943)

$$h_c = \frac{2c}{\gamma\sqrt{K_a}} \quad (14)$$

where K_a = lateral earth pressure coefficient will intersect the slope BC at D. The presence of vegetation, in particular tree roots, would increase the depth of the vertical face. Capillarity can also result in the formation of vertical faces on the sandbars. However, such faces will be unstable when the sandbar face is fully inundated.

The surfaces ABC or ABDE define the upper limit for slope stability under seepage and can be further degraded by rilling, tractive, wave, and other erosion processes. The soil within either of these surfaces and the maximum depositional slope constitutes sediments that would be in a state of flux undergoing cyclic accretion and erosion.

The intersection of AB and BC depends on the location of the ground-water level at peak river stage. We define the height of this intersection, above the low water level, as βH_w , where H_w is the maximum height of river stage and β is a coefficient between 0 and 1. The coefficient β then depends on the location of the ground-water level. There are various methods available for the prediction of the ground-water level for unconfined seepage flows. The differences between the methods come from the solution techniques used in solving the governing equation involving Darcy's law and continuity. Apart from problems with very simple geometry, where closed-form solutions may be found, these methods employ numerical techniques—finite-difference method, finite-element method, and boundary-element method. Finite-element (Taylor and Brown 1967; Neuman and Witherspoon 1971; Neuman 1973; Desai 1976; Bathe and Khoshgoftaar 1979; Desai and Li 1983; Lacy and Prevost 1987) and boundary element methods (for example, Liggett 1977) are becoming the methods of choice. Two schemes are often used in the finite-element method: one called the variable mesh method, the other called an invariant or constant mesh or fixed mesh procedure. An examination of the differences between and modifications of these schemes is presented by Cividini and Gioda (1989).

In transient problems, each cycle of infiltration and seepage will incur stress changes that may influence the location of the ground-water surface in certain types of soils, especially soft normally consolidated clays. A fall in river stage would cause a decrease in the hydrostatic pressure on the face of the riverbank and a decrease in pore-water pressure within the bank with a concomitant increase in effective stresses. The soil will consolidate and the permeability will decrease. A rise in river stage would incur the opposite. In the conventional approach to ground-water problems, the stress changes are not coupled to the flow equations.

In determining the ground-water level and the coefficient β , we used a constant mesh finite-element scheme to solve Biot's (1941) coupled consolidation analysis modified to separate the compression of soil solids from the pore water as

$$k_x \frac{\partial^2 h}{\partial x^2} + k_y \frac{\partial^2 h}{\partial y^2} + k_z \frac{\partial^2 h}{\partial z^2} = -\frac{\partial}{\partial t} \left(\epsilon_v + \frac{u}{K_w} \right) \quad (15)$$

where k_x, k_y, k_z = coefficients of permeability in the $x, y,$ and z Cartesian directions, respectively; h = head; ϵ_v = volumetric strain of the soil solids; u = pore-water pressure; K_w = bulk modulus of water; and t = time. The volumetric strains of the soil is found using appropriate constitutive soil models. In our case, we assumed that the soil undergoes elastic deformation consistent with the modified Cam-clay model (Roscoe and Burland 1968). Eq. (15) with the modified Cam-clay model was coded for a two-dimensional case with isotropic permeability, into an algorithm using standard finite-element coding (Smith and Griffith 1988; Budhu and Wu 1992).

EFFECTS OF RISING RIVER STAGE

Various rates of rise of river stage (r) were imposed on a sandbar with a slope (α) of 26° and a permeability (k) of 1×10^{-5} m/s. The predicted phreatic surfaces are shown in Fig. 6 together with the stable seepage slope. A plot of the variation of the coefficient β with rate of rise of river stage (extracted from Fig. 6) shows that β increases rapidly for $r < 0.1$ m/h and reduces gradually for $r > 0.1$ m/h (Fig. 7). The transition rate of rise river stage, $r = 0.1$ m/h, is about three times the coefficient of permeability. Thus, it appears that dam discharges that produce river stage rise less than three times the permeability of sandbars are likely to affect a larger area of the sandbar than faster rate of river stage rise ($r > 3k$). However, the changes in β are small for common rates of rise (0.3 to 0.5 m/h) of river stage downstream of the Glen Canyon Dam. Approximate relationships between β and rate of rise of river stage are

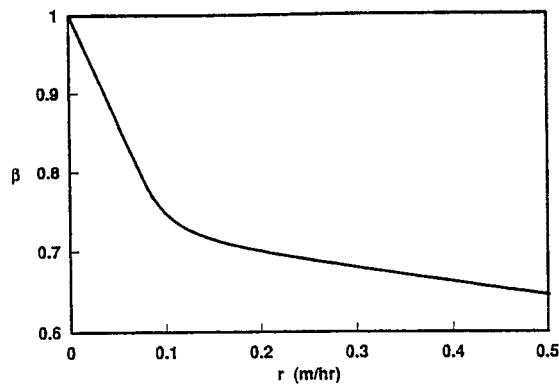


FIG. 7. Variation of β with r

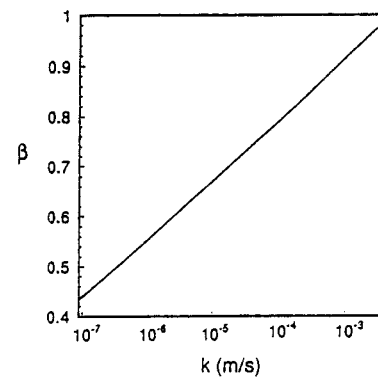


FIG. 8. Variation of β with k

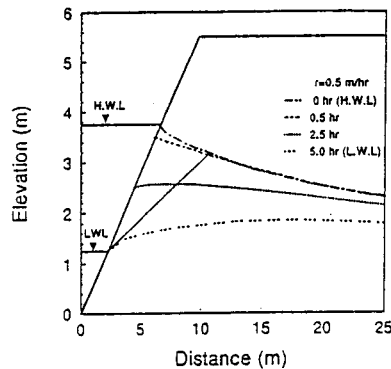


FIG. 9. Effect of Falling River Stage on Phreatic Surface

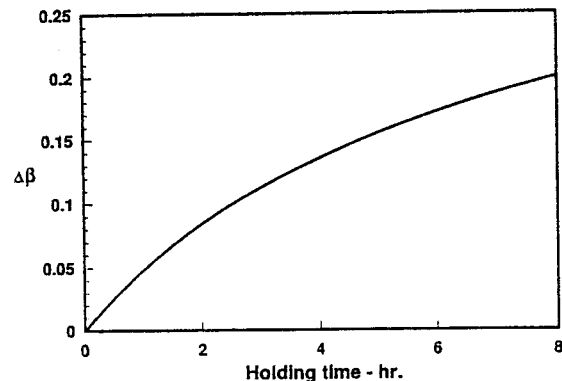


FIG. 10. Variation of β with Holding Time

$$\beta = 1.0 - 2.4r; \quad r < 0.1 \text{ m/h}; \quad \beta = 0.774 - 0.167r; \quad r > 0.1 \text{ m/h} \quad (16, 17)$$

EFFECTS OF PERMEABILITY

A second set of analyses was conducted by varying the coefficient of permeability keeping the slope and the rate of rise of river stage constant at 26°C and 0.25 m/h respectively. The parameter β was found to vary linearly with the natural logarithm of the permeability (Fig. 8). It is expected that with higher permeabilities, the parameter β would increase as obtained from the analysis. Thus, a larger mass of soil would be involved in bank cuts if the permeability of the soil increases. An approximate relationship between β and permeability is given by

$$\beta = 1.4 + \ln(k) \quad (18)$$

EFFECTS OF SLOPE ANGLE

A third set of analyses was conducted in which the slope angle was varied but the coefficient of permeability and the rate of rise of river stage were kept constant at $1 \times 10^{-4} \text{ m/s}$ and 0.25 m/h respectively. It was found, within practical ranges of slope angles corresponding to the angles of internal friction of cohesionless materials, that slope angle does not have a significant effect on the parameter β compared to the coefficient of permeability. The relationship between β and slope angle can be approximated as

$$\beta = 1.32 - 0.12 \ln(\alpha) \quad (19)$$

EFFECTS OF FALLING RIVER STAGE

If the river stage falls slowly, water can still infiltrate the sandbar causing the elevation of a part of the phreatic surface, away from the face of the sandbar, to rise. The time for the Glen Canyon Dam to lower the discharge from peak discharge to its lowest discharge, on any given day, varies between 4 h and 16 h. However, the time for the river stage to fall from high water level to low water level varies with location. Average rate of fall of river stage, calculated from data collected by Carpenter et al. (1992), varies between 0.25 m/h and 0.5 m/h .

The effects of rate of fall of river stage ranging from 0.25 m/h were analyzed for a sandbar with different permeabilities and slope angles. A typical result of the movement of the phreatic

surface during falling river stage is shown in Fig. 9. The results reveal that β is insensitive to the rate of fall of river stage. However, from geotechnical principles, a rapid rate of drawdown could lead to severe bank cuts from undrained slope failures, but the "simple" model in this contribution cannot account for this condition.

COMBINED EFFECTS OF RISING AND FALLING RIVER STAGE, SOIL PERMEABILITY, AND SLOPE ANGLE

Equations (16)–(19) only give the relationship between β and each of the parameters, rate of rise of river stage, soil permeability, and slope angle. Using optimization methods, approximate general expression for β are

$$\beta = 1.308 - 0.072 \ln \left(\frac{r}{k} \right) - 0.132 \ln(\alpha); \quad \frac{r}{k} > 1, \alpha > 10.5^\circ \quad (20)$$

$$\beta = 1.0 - 0.065 \ln \left(\frac{r}{k} \right) - 0.128 \ln(\alpha); \quad \frac{r}{k} < 1, \alpha > 10.5^\circ \quad (21)$$

It was shown in the preceding that β is insensitive to rate of fall of river stage (d) downstream from the Glen Canyon Dam. Eq. (20) and (21) can be used to determine β to delineate the lower stable seepage slope and to estimate the mass of sediments that would undergo cyclic seepage erosion and aggradation under transient flow.

EFFECTS OF PEAK DISCHARGE HOLDING TIME

If the dam discharge regime is such that the peak discharge is held constant for a period longer than an instantaneous peak, then the phreatic surface position will rise. The area affected by seepage erosion will also increase. The effects of peak discharge holding time were investigated for sandbars with slopes ranging from 12° to 32° , soil permeability ranging from 1.0×10^{-3} to 1.0×10^{-7} m/s and holding times ranging from 0 h to 8 h.

The value of β was found to increase rapidly during the first 2 h of the holding period and then to increase at a slower rate for longer holding times (Fig. 10). At the beginning of the holding period, a large difference in head exists across the sandbar. However, as the holding period increases, water entering the sandbar causes the phreatic surface to rise, resulting in a decrease in the head with time. The net result is a decrease in the rate of change of β with time. Using optimization techniques, the change of β with permeability, slope, and holding time is given as follows.

For $P_t \leq 2$ h

$$\Delta\beta = 0.085 - 30k + 0.003\alpha + 0.045P_t \quad (22)$$

For $P_t > 2$ h

$$\Delta\beta = 0.130 + 40k + 0.006\alpha + 0.020P_t \quad (23)$$

The position of the phreatic surface for holding time greater than zero is obtained by adding β from equation (20) or (21) to $\Delta\beta$ from the appropriate holding time equation [(22) or (23)].

WIDTH OF SANDBARS AFFECTED BY SEEPAGE

The concern for riparian habitat and recreation use would be the height and width of the affected region. From the geometry of Fig. 5, the width w (inset diagram Fig. 11) is

$$w = \beta H_w \cot \alpha + (H - \beta H_w) \cot \phi' - H \cot \phi' = \beta H_w (\cot \alpha - \cot \phi') \quad (24)$$

By substituting (13) into (24), we obtain

$$w = \beta H_w \frac{\gamma_w}{\gamma_{sat}} \cot \phi' \quad (25)$$

As a first approximation, for most common soils, $\gamma_{sat}/\gamma_w \approx 2$ and

$$w = \frac{\beta H_w}{2} \cot \phi' \quad (26)$$

If the soil has some cohesion, then

$$w_1 = w - w_2 = \cot \phi' \left(\beta H_w \frac{\gamma_w}{\gamma_{sat}} - \frac{2c}{\gamma \sqrt{K_a}} \right) \quad (27)$$

where

$$w_2 = \frac{2c}{\gamma \sqrt{K_u}} \cot \phi' \quad (28)$$

The variation of the angle of internal friction of the soil with the width, w , normalized to the fluctuation depth for $\gamma_{sat}/\gamma_w \approx 2$ and $\gamma_{sat}/\gamma_w \approx 2.5$ is shown in Fig. 11. The latter value is the average value from density measurements from three sandbars downstream from the Glen Canyon Dam.

COMPARISON OF ANALYSIS WITH FIELD DATA

During the two-year study period, the U.S. Bureau of Reclamation conducted a series of test flows to determine how dam operations affect downstream sandbar deposits and biomass in the Colorado River. Scientists from Northern Arizona University surveyed twenty-nine sandbars (Beus et al. 1992) before and after the test flows. Each sandbar was divided into 8 or more transects and each transect was surveyed before and after each test flow. River stage, groundwater levels, water temperatures, and tilts were monitored on three sandbar sites (-6.5R, 43L and 172L; Fig. 1) by the U.S. Geological Survey (Carpenter et al. 1992). Events on one sandbar (sandbar 172L) will be described to depict some of the changes that are occurring.

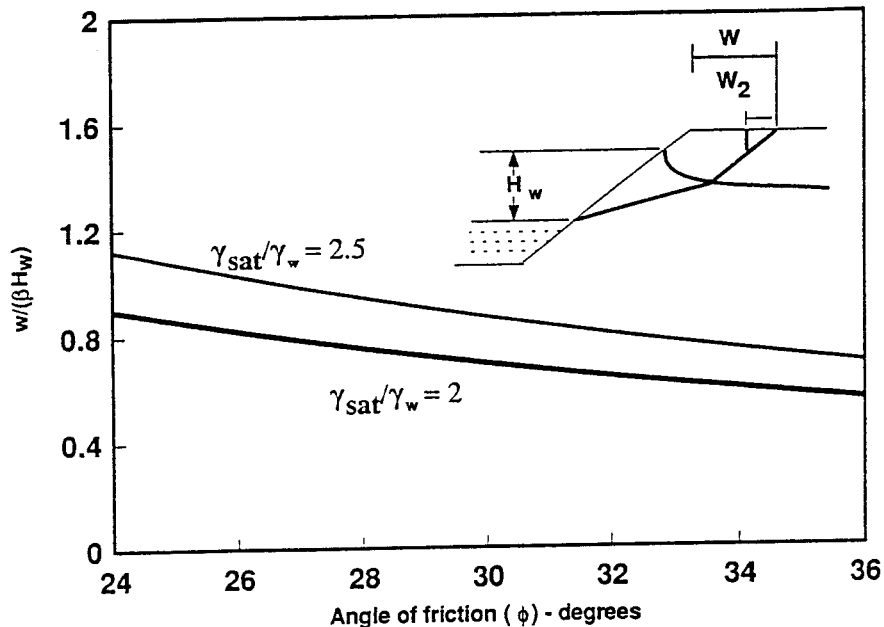


FIG. 11. Reduction of Width of Sandbars with Angle of Friction

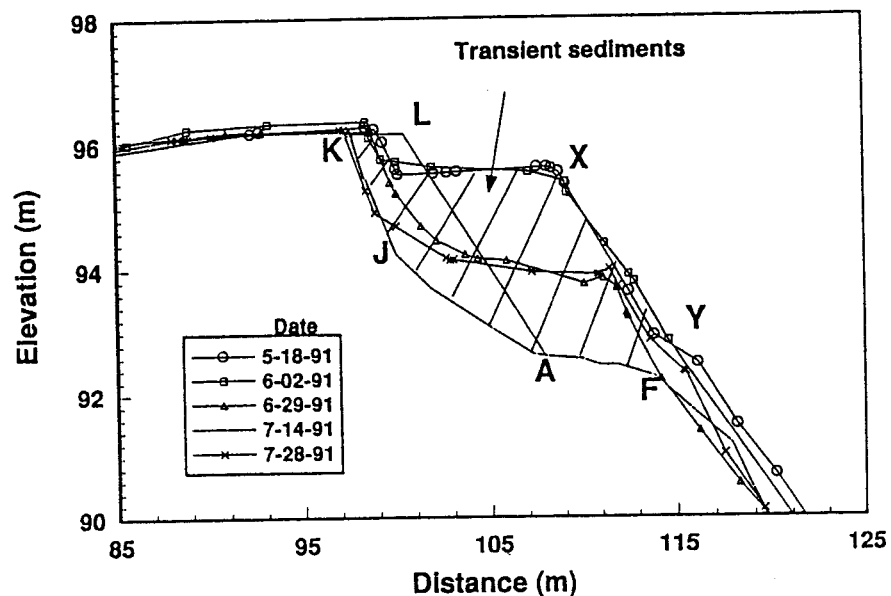


FIG. 12. Changes of Cross Section at Sandbar 172L as Determined by Ground Surveys

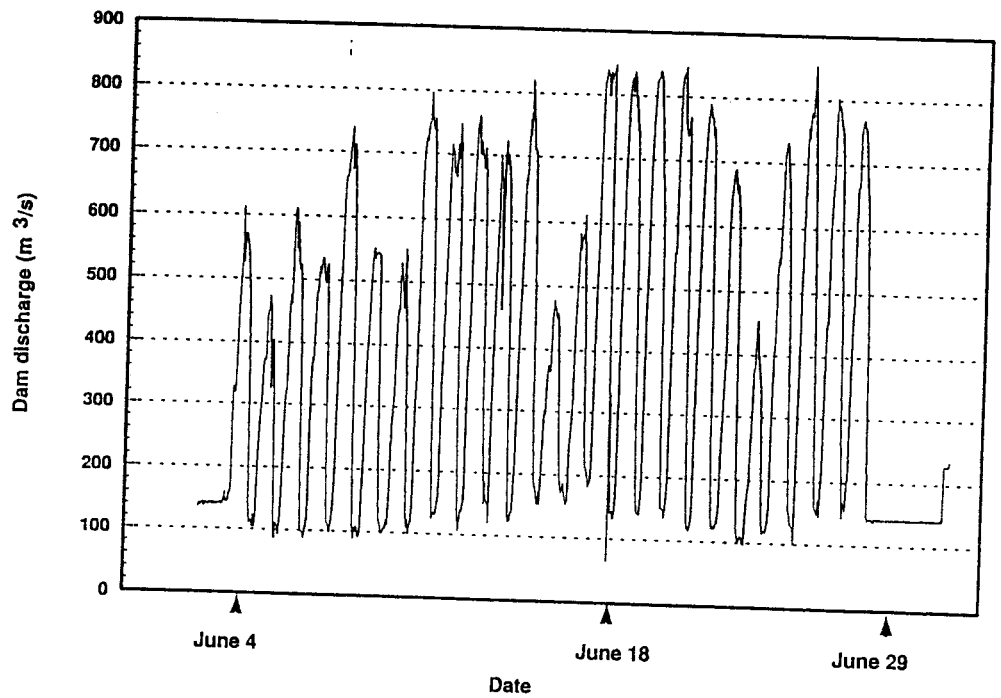


FIG. 13. Dam Discharge during June 1991

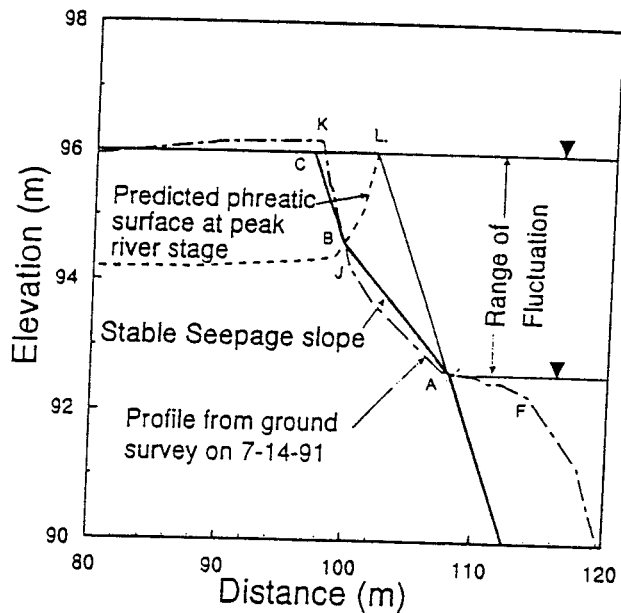


FIG. 14. Comparison of Stable Seepage Slope with Field Data for Sandbar 172L

Sandbar 172L is located 277 km downstream from Lees Ferry, Ariz. (Fig. 1). This sandbar was and is very active. It grew outward from approximately the slope AL and then exhibited several cycles of erosion and aggradation within an active region (hatched area, Fig. 12) during the study period. The unit weight of the sand in the active region is 16 kN/m^3 compared with the stable region (unshaded) of 17.2 kN/m^3 . The angle of friction of the sand, determined from shear box tests is 26° , for the active region and 32° for the stable region. Falling head field permeability tests, conducted using the variable head borehole method described by Hvorslev (1951), gave a coefficient of permeability, $k = 2.3 \times 10^{-4} \text{ m/s}$.

On June 4, 1991, a 27-day test flow was released from the Glen Canyon Dam. The hydrograph was intended to replicate widely fluctuating summer flows. The minimum discharge was $68 \text{ m}^3/\text{s}$ and the maximum was $836 \text{ m}^3/\text{s}$ with a mean value of $380 \text{ m}^3/\text{s}$ (Fig. 13). Prior to this test flow, ground surveys (Beus et al. 1992) on May 18 and June 2, 1991 showed that sandbar 172L had a maximum slope XY of 26° (Fig. 12). On June 18, a slope failure involving sediments between XY and FAJK (Fig. 12) was observed at low river stage (Cluer 1992). By June 19, 1991, a ground survey indicated that the sandbar returned to an aggradational mode. Subsequent observations of sandbar 172L reveal a pattern of slope failures up to FAJK, followed by aggradation.

TABLE 1. Comparison of Predicted Stable Seepage Slopes with Field Data

Sandbar (1)	Slope AB (2)	Slope BC (3)
3	13.88	32.11
6	10.93	30.14
16	9.66	32.26
30	13.32	27.11
31	13.50	30.12
43	19.87	32.81
45	13.92	31.35
47	11.31	29.73
50	13.70	31.12
51	13.99	29.12
68	9.95	25.63
81	10.51	30.08
91	12.57	31.96
93	9.80	31.48
104	15.13	32.62
119	11.20	32.60
122	9.83	28.46
123	6.24	31.91
137	8.13	32.77
145	9.2	27.53
172	10.51	28.17
183	8.71	33.11
194	7.21	28.95
203	7.12	28.80
213	8.56	28.18
220	8.10	31.21
[Average slope]	11.17	30.33
[Standard deviation]	2.93	2.07
[Predicted]	11-14	27-32

Measurements of river stage variations during this period (Carpenter et al. 1992) showed that the average rate of river stage rise was 1.128×10^{-4} m/s. We assumed that the area bounded by AJKLA comprised the transient sediments prior to the test flows during the two-year study period. Substituting the appropriate values ($r = 1.128 \times 10^{-4}$ m/s, $k = 2.3 \times 10^{-4}$ m/s, and $\alpha = 26^\circ$) for this sandbar in (21) gives $\beta = 0.63$ and from (13), $\alpha_s = 12.7^\circ$ for $D = 0$, $\gamma_{sat} = 16$ kN/m³. The lower stable seepage slope (AB) is then 12.7° and the upper stable seepage slope (BC) is $\phi' = 32^\circ$. The predicted equilibrium seepage surface, ABC, shows very good agreement with the lowest measured profile, AJK, as shown in Fig. 14. Once a Coulomb-type failure has occurred, failure planes such as ABC become the preferred planes of failure. That is, sediments aggradating on planes such as ABC will be unstable and will fail along these planes from seepage forces.

The complete set of ground survey data from 28 sandbars monitored during the two-year period (Beus et al. 1992) was used to further validate the simple analysis. The minimum lower seepage slope (AB) above the low water level and the maximum upper seepage slope (BC) were extracted from each of the profiles surveyed by Beus et al. (1992). For each sandbar, the average value of these slopes for each transect was calculated and then the average over all the transect was computed. The results are shown in Table 1. The predicted values of the equilibrium slopes based on the range of soil properties measured (Budhu 1992) are compared with the average value for 28 of the 29 sandbars at the bottom of Table 1. The field data are within the range of values predicted by the analysis for the range of soil properties measured on three sandbars. One sandbar, sandbar 8, has only a single slope and was excluded from Table 1.

CONCLUSIONS

The simple analysis proposed in the present paper could be used to predict, as a first approximation, the stable seepage sandbar face that could be attained under fluctuating river stages. It was established that seepage parallel to the slope is the limiting condition for a Coulomb-type failure. Three factors—range of river stage fluctuation, rate of rise of river stage, and soil permeability—control the amount of sediments involved in seepage erosion. The larger the range of fluctuation, rate of rise of river stage, and permeability, the greater the active zone of seepage erosion. Sediments, enclosed by this stable seepage slope and the maximum slope angle, will undergo cyclic aggradation and erosion depending on the dam discharged regimes, the local hydraulic conditions and the availability of sediments. The cyclic pattern of erosion (slope failures) and aggradation that is evident on many of the sandbars downstream from the Glen Canyon Dam involves transient sediments deposited during favorable hydraulic and hydrologic conditions.

ACKNOWLEDGMENTS

The writers wish to thank the Glen Canyon Environmental Studies for the financial support of this research. The ground survey data was supplied to us by S. Bues and M. Kaplinski of Northern Arizona University. M. Carpenter and Rob Carruth of the U.S. Geological Survey provided the river stage data near sandbar 172L. Brian Cluer of the Glen Canyon Environmental Studies provided details of failures captured by time-lapsed photography. The writers thank the aforementioned scientists for the information provided and also Larry Stevens and Dave Wegner from the Glen Canyon Environmental Studies, and Bill Jackson and Rick Inglis from the National Park Service. The writers thank William Rasmussen for reviewing the draft of this paper. This paper does not necessarily reflect the views of the Glen Canyon Environmental Studies.

APPENDIX I. REFERENCES

- Bathe, K. J., and Khoshgoftaar, M. R. (1979). "Finite element free surface seepage analysis without mesh iteration." *Int. J. Num. Anal. Methods Geomech.*, 3, 13-22.
- Beus, S. S., Avery, C. C., Stevens, L. E., Kaplinski, M. A., Mayes, H. B., and Cluer, B. L. (1992). "The influence of variable discharge regimes on Colorado River sand bars below Glen Canyon Dam." *The influence of variable discharge on Colorado River sand bars below Glen Canyon Dam: final report*, S. S. Beus and C. C. Avery, eds., National Park Service, Flagstaff, Ariz.
- Biot, M. A. (1941). "Theory of elasticity and three dimensional consolidation." *J. of Appl. Physics*, 12, 155-164.
- Budhu, M. (1992). "Mechanisms of erosion and a model to predict seepage erosion due to transient flow." *The influence of variable discharge on Colorado River sand bars below Glen Canyon Dam: final report*, S. S. Beus and C. C. Avery, eds., National Park Service, Flagstaff, Ariz.
- Budhu, M., and Wu, C. S. (1992). "Numerical analysis of sampling disturbances in clay soils." *Int. J. Num. Anal. Methods Geomech.*, 16, 467-492.
- Carpenter, M. C., Carruth, R. L., Fink, J. B., Boling, J. K., and Cluer, B. L. (1992). "Hydrogeology of beaches 43.1L and 172.3L and the implications on flow alternatives along the Colorado River in the Grand Canyon." *The influence of variable discharge on Colorado River sand bars below Glen Canyon Dam: Final report*, S. S. Beus and C. C. Avery, eds., National Park Service, Flagstaff, Ariz.
- Cividini, A., and Gioda, G. (1989). "On the variable mesh finite element analysis of unconfined seepage problems." *Géotechnique*, 2, 251-276.
- Cluer, B. L. (1992). "Daily responses of Colorado River sandbars to Glen Canyon Dam tests flows, Grand Canyon, Arizona, and analysis of sand bar response along the Colorado River in Glen and Grand Canyons to test flows from Glen Canyon Dam, using aerial photograph." *The influence of variable discharge on Colorado River sand bars below Glen Canyon Dam: final report*, S. S. Bues and C. C. Avery, eds., National Park Service, Flagstaff, Ariz.
- Desai, C. S. (1976). "Finite element residual schemes for unconfined flow." *Int. J. Num. Meth. Engrg.*, 5, 1415-1418.
- Desai, C. S., and Li, G. C. (1983). "A residual flow procedure and application for free flow in porous media." *Adv. in Water Resour.*, 6, 27-35.
- Howard, A. D., and Dolan, R. (1981). "Geomorphology of the Colorado River in the Grand Canyon." *J. Geol.*, 89, 269-298.
- Howard, A. D., and McLane, C. F. (1988). "Erosion of cohesionless sediment by groundwater seepage." *Water Resour. Res.*, 24, 1659-1674.
- Hvorslev M. J. (1951). "Time lag and soil permeability in groundwater observations." *Bulletin 36*, Waterways Experiment Station, U.S. Army Corps of Engineers, Vicksburg, Miss.
- Lacy, S. J., and Prevost, J. H. (1987). "Flow through porous media: a procedure for locating the free surface." *Int. J. Num. Anal. Methods Geomech*, 11(6), 585-601.
- Liggett, J. A. (1977). "Location of free surface in porous media." *J. Hydr. Div., ASCE*, 103(4), 353-365.
- Neuman, S. P. (1973). "Saturated-unsaturated seepage by finite element method." *J. Hydr. Div., ASCE*, 99(12), 2233-2251.
- Neuman, S. P., and Witherspoon, P. A. (1971). "Analysis of non-steady flow with a free surface using the finite element method." *Water Resour. Res.*, 7(3), 611-623.
- Roscoe, K. H., and Burland, J. B. (1968). "On the generalized stress-strain behavior of a wet clay." *Engineering plasticity*, J. Heyman and F. A. Lechie, eds., Cambridge University Press, Cambridge, U.K., 535-609.
- Schmidt, J. C., and Graf, J. B. (1990). "Aggradation and degradation of alluvial sand deposits 1965 to 1986, Colorado River, Grand Canyon National Park, Arizona." *Paper 1493*, U.S. Geological Survey, Washington, D.C.
- Smith, I. M., and Griffith, D. V. (1988). "Programming the finite element method." 2nd ed., John Wiley and Sons, Ed., New York, N.Y.
- Stevens, L. (1983). *The Colorado River in the Grand Canyon, a guide*. Red Lake Books, Flagstaff, Ariz.
- Taylor, D. W. (1948). *Fundamental of soil mechanics*. John Wiley & Sons, New York, N.Y.
- Taylor, R. L., and Brown, C. B. (1967). "Darcy flow solution with a free surface." *J. Hydr. Div., ASCE*, 93(2), 25-33.
- Terzaghi, K. (1943). *Theoretical soil mechanics*, John Wiley and Sons, New York, N.Y.
- Turner, R. M., and Karpisak, M. M. (1980). "Recent vegetation changes along the Colorado River between Glen Canyon Dam and Lake Mead, Arizona." *Professional Paper 1132*, U.S. Geological Survey, Washington, D.C.
- U.S. Department of the Interior Bureau of Reclamation. (1988). *Glen Canyon environmental studies final report*, Washington, D.C.

APPENDIX II. NOTATION

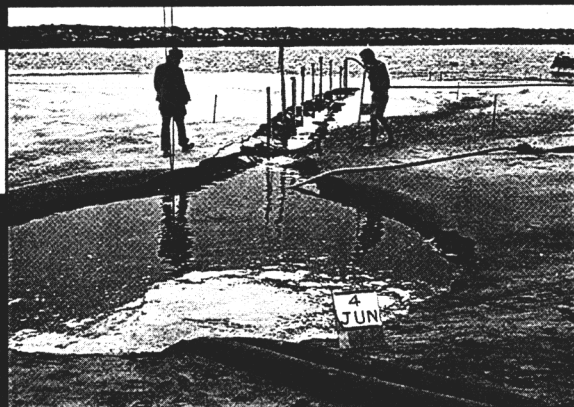
The following symbols are used in this paper:

- c = cohesion;
 D = depth of unsaturated zone;

D_{50} = mean grain diameter;
 e = void ratio;
 F = factor of safety;
 G = specific gravity of soil;
 H_w = maximum range of river stage fluctuation;
 h = depth below ground-water surface and head;
 h_c = depth of tension crack;
 i = hydraulic gradient;
 K_a = coefficient of lateral active earth pressure;
 K_w = bulk modulus of water;
 k_x, k_y, k_z = coefficient of permeability in x, y, z Cartesian coordinate system;
 N = normal force;
 P_t = peak holding time;
 r = rate of rising river stage;
 S = degree of saturation;
 T = force down slope;
 t = time;
 u = pore-water pressure;
 W = weight;
 w = width;
 α = slope angle;
 α_s = stable seepage slope;
 γ = bulk unit weight;
 γ_{sat} = saturated unit weight;
 γ_w = unit weight of water;
 γ' = effective unit weight;
 λ = direction of seepage vector with plane normal to slope; and
 ϕ' = effective angle of internal friction.

JAN./FEB. 1995 VOL. 121 NO. 1
ISSN 0733-9437
CODEN: JIDEDH

JOURNAL OF IRRIGATION AND DRAINAGE ENGINEERING



AMERICAN SOCIETY OF CIVIL ENGINEERS
WATER RESOURCES ENGINEERING DIVISION

TECHNICAL PAPERS

- Brooks-Corey and van Genuchten
Soil-Water-Retention Models
**J. M. Stankovich and
D. A. Lockington** 1
- Ground-Water Flow into
Nonpenetrating Well
**Kamala K. Singh,
Shambhu P. Dasgupta,
Akhilesh P. Mishra, and
Triveni P. Ojha** 8
- Seepage Erosion from Dam-Regulated
Flow: Case of Glen Canyon
Dam, Arizona
Muniram Budhu and Roger Gobin 22
- Use of Flood-Control Reservoirs for
Drought Management
**Tiao J. Chang, Xenia A. Kleopa, and
Choo B. Teoh** 34
- Automatic Irrigation Scheduling
System (AISSUM): Principles
and Applications
**Bhawan Singh, Jean Boivin,
Glenn Kirkpatrick, and Barry Hum** 43
- Intake Parameters from Advance and
Wetting Phases of Surface Irrigation
**Edmar J. Scaloppi, Gary P. Merkley,
and Lyman S. Willardson** 57
- Irrigation-Drainage Design and
Management Model: Development
**Luis A. Garcia, Henry B. Manguerra,
and Timothy K. Gates** 71
- Irrigation-Drainage Design and
Management Model: Validation
and Application
**Henry B. Manguerra and
Luis A. Garcia** 83
- Estimating Hydraulic Conductivity for
Models of Soils with Macropores
Mahmood H. Nachabe 95

TECHNICAL NOTES

- Assessment of Streamflow
Augmentation in Case of Weakly
Dependent Data
**Arie Ben-Zvi and
Margarita Langerman** 104
- Effect of Surface Source Variation on
Seawater Intrusion in Aquifers
A. Mahesha and S. H. Nagaraja 109
- Defining Furrow Cross Section
Joel E. Cahoon 114